Carbohydrate Polymers 88 (2012) 576–582

Contents lists available at SciVerse ScienceDirect

Carbohydrate Polymers

journal homepage: www.elsevier.com/locate/carbpol

Synthesis and characterization of carboxymethyl chitosan carrying ricinoleic functions as an emulsifier for azadirachtin

Bo-Hua Feng, Liu-Fen Peng*

College of Medical Information Engineering, Guangdong Pharmaceutical University, Guangzhou 510006, China

ARTICLE INFO

Article history:
Received 3 October 2011
Received in revised form
30 December 2011
Accepted 1 January 2012
Available online 8 January 2012

Keywords:
Chitosan derivative
Azadirachtin
Nanocarrier

ABSTRACT

An amphiphilic carboxymethyl chitosan with ricinoleic acid (R-CM-chitosan) was synthesized, and was used as a carrier for the botanical pesticide azadirachtin (Aza), which formed a Aza/R-CM-chitosan water dispersion on the nanoscale level. The shape, zeta potential, loading efficiency and outdoor stability of the Aza/R-CM-chitosan nanoparticle were characterized. The relationship between the nanoparticle's performance and the constituents' concentrations in a water-dispersion was discussed. The results indicated that the nanoparticle's size, polydispersity index and zeta potential were all influenced by the concentration ratio of the carrier to the drug, especially for ratios between 5 and 15. The Aza/R-CM-chitosan nanoparticle had a small (200–500 nm) and polydisperse particle size, with a negative charge on the particle surface. R-CM-chitosan efficiently restrained Aza degradation in a natural environment, as the loading efficiency reached up to 56%. Furthermore, Aza/R-CM-chitosan provided a better controlled release of the drug compared to the control groups.

1. Introduction

Water dispersed pesticide formulations are considered environmentally friendly, and most lipid-soluble compounds can be solubilized into water depending on the use of various surfactants. In many respects, polymer surfactants are considered superior, particularly when compared to small molecule surfactants. Polymer surfactants with hydrophobic groups on the polymer chain have much better loading capacity of lipophilic compounds, such as some pesticides, which can improve the stability of the water dispersion and allow a controlled release of pesticides. As such, biodegradable polymer surfactants could provide improved environmental protection. Chitosan is the only biodegradable cationic polysaccharide, having the correct pharmacological activity and growth regulation for crops (Muzzarelli et al., 2011). Chitosan derivatives were developed to improve chitosan's poor solubility in neutral water (pH = 7). For example, when modified with a hydrophobic group, chitosan could be a good self-aggregating carrier for lipid-soluble drugs (Shen & Song, 2009). However, lipid-soluble pesticides were conventionally dispersed in a highly toxic solvent and additives to produce formulation such as an emulsion, an emulsifiable concentrate and a suspension concentrate. The pesticide's particle size in such formulations was usually much larger (around 2 μm) than those found in the nanoscale range. Furthermore, a nanopesticide provided improved bioavailability of the pesticide, due the combined attributes of a large surface area and small particle size (Shenoy & Sukhorukov, 2004). Liu, Tong, and Prud'homme (2008) prepared a water-dispersed crystalline grain of pesticide in nanoscale, and Guan, Chi, Yu, and Li (2008) coated a nanoscale pesticide grain with synthesized polymers, which preserved the pesticide for a controlled release.

The scope of this paper is to demonstrate the usefulness of the modified chitosan, a novel water-soluble derivative of chitosan and ricinoleic anhydride, in formulating aqueous dispersions together with the botanical lipid-soluble pesticide azadirachtin (Aza). Carboxymethyl chitosan with ricinoleic acid (R-CM-chitosan) was synthesized. The reaction conditions were investigated and the reaction products were characterized. Aza was then loaded onto R-CM-chitosan to form a Aza/R-CM-chitosan water dispersion, wherein the Aza degradation could be evaluated in a natural environment, and compared with the small molecule carrier R-Na (sodium ricinoleate). The Aza/R-CM-chitosan particles size, polydispersity index (PDI), zeta potential, morphological structure, components concentration relations and loading efficiency (LE) would be shown. The approaches used to control the performance of Aza/R-CM-chitosan water dispersion were also discussed in detail.

2. Experimental

2.1. Materials and instrument

6-O-carboxymethyl chitosan (6-O-CM-chitosan) whose degree of carboxymethylation was 0.64, ricinoleic anhydride (R) and

* Corresponding author. Tel.: +86 20 84519177; fax: +86 20 38212207.
E-mail addresses: bandi-01@163.com, tfengbh@163.com (L.-F. Peng).

0144-8617/$ – see front matter © 2012 Elsevier Ltd. All rights reserved.
doi:10.1016/j.carbpol.2012.01.002

sodium ricinoleate (R-Na) were prepared by the polymers laboratory of the department of materials science and engineering at Jinan University (Guangzhou, China). An azadirachtin standard was purchased from Sigma (USA), and azadirachtin was obtained from the Jiaxing chemistry factory (98% pure, Fengshun of Guangdong, China). All other reagents were analytical grade and were used directly without further purification. All solvents and water were redistilled freshly.

2.2. Synthesis of carboxymethyl chitosan with ricinoleic acid (R-CM-chitosan)

The CM-chitosan degree of substitution (DS) was determined by potentiometric titration (Ge & Luo, 2005), and the structure of the CM-chitosan was characterized by Fourier transform infrared spectroscopy (FTIR, Equinox55, Bruk, Germany). CM-chitosan samples were dispersed in pyridine into which NaI had been previously dissolved. The R was then added dropwise to the mixture with magnetic stirring and then allowed to react at temperatures between 40 °C and 100 °C for 6 h (Scheme 1).

The molar ratios of R to the primary amino of the CM-chitosan, for the reactions, were 1:1, 3:1 and 5:1. The reaction products were rinsed in ethanol and acetone 5 times and dried at 60 °C under vacuum for 48 h. FTIR was used to determine structure of reaction products. The DSs of R were calculated after carbon and nitrogen elemental analysis (EA2400II, Perkin-Elmer, USA). The molecular weight of R-CM-chitosan samples with higher DS were measured by ubbelohde viscometer, which samples were dissolved in 0.1 M NaAc aqueous solution under 30 °C (Nishimura, Nishi, & Tokura, 1986).

2.3. Preparation of Aza/R-CM-chitosan water dispersion

The samples of R-CM-chitosan were dissolved in deionized water (pH = 6.8) to obtain the carrier solution (10 mg/ml). The Aza solution was then blended with the carrier solutions of given concentrations to form Aza/R-CM-chitosan water dispersions under 200 rpm stirring by magnetic stirring apparatus (85-2, Xingchen Instruments, China) at room temperature for 30 min, where the Aza concentrations ranged from 0.20 to 0.20 mg/ml separately.

2.4. Characterization of Aza/R-CM-chitosan water dispersion

The solubility of R-CM-chitosan in aqueous was observed under variant pH values, which were adjusted by dissolving 0.2 g R-CM-chitosan in HCl (20 ml, 0.1 M) with NaOH (0.1 M) titration. And the pH values were then measured and recorded by pH meter (PHS-3C, Sheng Ci Instruments, Shanghai, China).

The samples of R-CM-chitosan and R-Na were diluted by deionized water (pH = 6.8), concentrations ranging from 0.1 to 10 mg/ml. Then intensities of light scattering of the samples solutions were measured by dynamic light scattering (DLS, BI-200SM, Brookhaven, USA) to study self-aggregation behavior of R-CM-chitosan conjugates. And the contact angles of R-CM-chitosan samples were measured by contact angle meter (CAM-PLUS, ANTEC, Germany). The surface tensions of Aza/R-CM-chitosan water dispersion samples were determined by surface tension meter (BZY-1, Heng Ping Instruments, Shanghai, China).

Ultracentrifugation of Aza/R-CM-chitosan was implemented by supercentrifuge (3K30, Sartorius-Sigma Laboratory Centrifuges, Germany) for 30 min (25,000 rpm, 4 °C), and the precipitate was collected for freeze-drying by freeze drier (FD1.0-60E, Heto, Denmark). The attenuated total reflectance (ATR) FTIR spectra of the Aza/R-CM-chitosan particles, the R-CM-chitosan and the Aza samples were then measured. The particle size, PDI and zeta potential were investigated with Zeta PALS (Brookhaven, USA). The particle morphological structure was demonstrated by scanning electronic microscope (SEM, XL-30E, Philips, the Netherlands) after dropping and drying the solutions onto base chips.

Table 1
Analysis on orthogonal test for R-CM-chitosan.

Test number	Factors				DS
	CM-chitosan	A/N	Pyridine	Temperature	
1	1	1	1	1	0.0414
2	1	2	2	2	0.0398
3	1	3	3	3	0.0450
4	2	1	2	3	0.1163
5	2	2	3	1	0.1297
6	2	3	1	2	0.1418
7	3	1	3	2	0.1464
8	3	2	1	3	0.1207
9	3	3	2	1	0.2526
Mean I	0.042	0.101	0.101	0.141	
Mean II	0.129	0.097	0.136	0.109	
Mean III	0.173	0.146	0.107	0.094	
Range	0.131	0.049	0.035	0.047	

The unloaded drug concentration in the supernatant of the Aza/R-CM-chitosan solution (1.5 ml) and LE was measured and calculated by the high performance liquid chromatography (HPLC, 1100, Agilent, USA). The chromatographic column used was a 250 mm × 4.0 mm, C18 reversed-phase column. The column temperature was 30 °C, and the mobile phase volume ratio acetonitrile:water = 7:3, with a flow velocity of 1.0 ml/min, a wavelength of 218 nm and a sampling volume 15 μL (Wu, Su, Zhang, & Lin, 2005).

2.5. Outdoor measurement of stability

Aza/R-CM-chitosan water dispersion was first prepared by Aza (0.10 mg/ml) and R-CM-chitosan (0.50 mg/ml). The control groups were prepared using the small molecule surfactant, R-Na and a water/acetone solution. The control groups were prepared with the same Aza concentration. Nylon sheets (size 20 cm × 20 cm per sheet) were either immersed in the water dispersion or the control groups. All sheets were dried outdoors in the sun for 11 days. The prepared nylon sheets were then immersed in methanol to leach the remaining Aza. The residual concentrations of Aza were measured by HPLC as described by Wu et al. (2005).

3. Results and discussion

3.1. Effects of reaction conditions on the degree of substitution (DS)

According to the principle reaction between anhydride and amide, a reaction mechanism was followed as shown in Scheme 1, where pyridine and NaI were used to prevent a hydrolysis reaction on the CM-chitosan molecule. The molecular weight of CM-chitosan, the molar ratios of R to primary amino (A/N), the reaction temperature and the amount of pyridine were all considered as factors for the reaction. Thus, an orthogonal test was carried out with 3 levels and 4 factors. The DSs of R in R-CM-chitosan molecules indicated that the molecular weight of CM-chitosan significantly influenced the R reaction with CM-chitosan according to the range in Table 1 and variance analysis in Table 2. Therefore, the preferred conditions for the reaction system tending to a higher DS of R (0.2526) were that low CM-chitosan viscosity-average molar mass (5.78×10^3), high A/N (5:1), mild reaction temperature (40 °C) and amount of pyridine less than 10% (v/v). And the molecular weight of the R-CM-chitosan samples with the higher DS (0.2526) was 9.60×10^3. Pyridine is often used to improve polymer solubility and maintain a homogeneous reaction system (Yi, Yang, Ying,

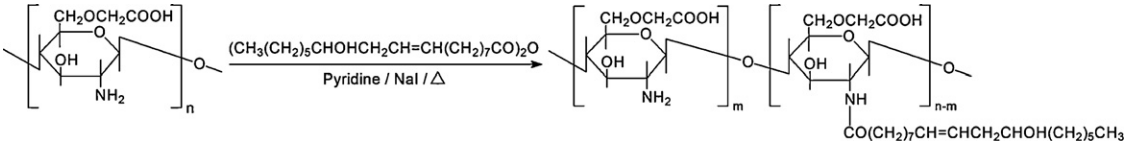

Scheme 1. Synthesis of R-CM-chitosan.

Table 2
Variance analysis on R-CM-chitosan.

Factors	S_T	f	F	F critical value ($\alpha = 0.05$)
Molecular weight	0.027	2	10.80[a]	6.940
A/N	0.005	2	2.00	6.940
Pyridine	0.002	2	0.80	6.940
Temperature	0.003	2	1.20	6.940

[a] Significant factors.

Chen, & Wang, 2006). Pyridine could also form N-acyl pyridinium salt with an anhydride, which would favor the acylation reaction. However, the pyridine concentrations reached a maximum during the reaction (Table 1), but by adding excessive pyridine the reaction proceeded and the reactants' concentrations decreased.

3.2. FTIR spectroscopy on R-CM-chitosan and Aza/R-CM-chitosan

FTIR spectra of CM-chitosan and R-CM-chitosan (Fig. 1a and b) showed O—H and N—H stretching vibration bands near 3427 cm^{-1} (Fig. 1b). This indicated that a substitution occurred at the —OH and —NH groups. Due to the substitution reaction occurring at the $—NH_2$ groups, the adsorption band of $—NH_2$ moved from 1597 cm^{-1} to 1560 cm^{-1}. The band at 1735 cm^{-1} represents an amide carbonyl made by the reaction. The characteristic absorption band of the C=C bond appeared at 3018 cm^{-1}, and C—H stretching vibration bands were identified at 2920 cm^{-1} and 2852 cm^{-1}, which were strong and sharply defined. A long carbon chain R was introduced into the CM-chitosan molecule successfully as confirmed by a band appeared around 720 cm^{-1} on the FTIR spectrum, which was identified as a $—(CH_2)_n$ group adsorption band ($n > 4$) of the R.

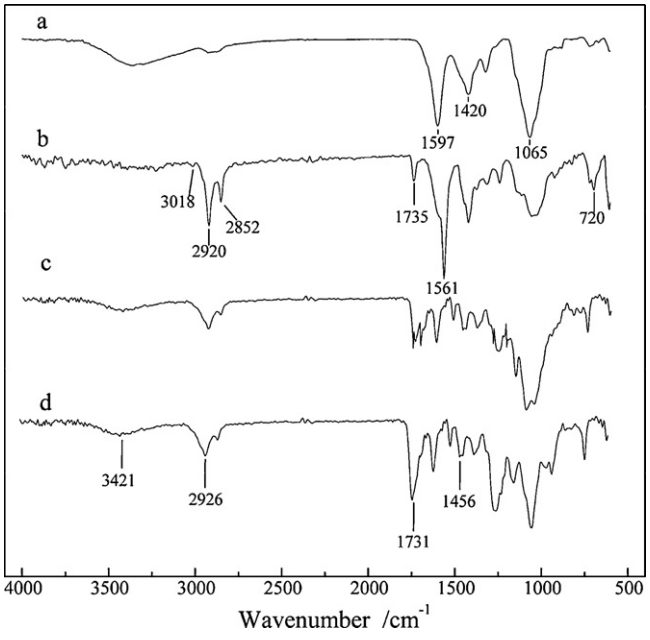

Fig. 1. FTIR spectra of (a) CM-chitosan, (b) R-CM-chitosan, (c) Aza/R-CM-chitosan and (d) Aza.

The FTIR spectra of Aza/R-CM-chitosan particle and Aza are shown in Fig. 1c and d, respectively. In the Aza/R-CM-chitosan spectrogram (Fig. 1c), the same main adsorption bands that were present in Fig. 1b remained, however, the intensity of the bands had weaken relatively. The band at 1731 cm^{-1} clearly demonstrated that there was a carbonyl group (C=O) associated with a Aza molecule. The changes detailed above indicated that Aza was efficiently loaded by carrier R-CM-chitosan.

3.3. Nanoparticles morphological structure

SEM photos of Aza/R-CM-chitosan particles are shown in Fig. 2. These were smooth, spherical particles of sizes primarily less than 500 nm, and they were well dispersed. Hydrophilic carboxymethyl trended toward the water phase while the hydrophobic R chain trended toward the oil phase to reduce surface tension, which formed shells of particles. Aza must have been effectively loaded into the carrier because the crystalline form of Aza was not readily observed.

SEM photos of Aza/R-CM-chitosan particles with a porous structure were also obtained (Fig. 2c), by drying the solution under 60 °C before SEM observation instead of drying at room temperature (Fig. 2a and b). The detail in Fig. 2c clearly demonstrates the core–shell structure of Aza/R-CM-chitosan particles. A model graph according to the self-consistent mean field theory (SCMFT) can be drawn as shown in Fig. 2d (He & Schmid, 2008), where green and gray, respectively represent hydrophobic and hydrophilic segments. It showed that the amphiphilic polymer could form a similar porous cage-shaped particle. It was inferred that the higher drying temperature would accelerate solvent evaporation, thus the shape of Aza/R-CM-chitosan particles in water dispersion was maintained after drying.

3.4. Solubility and self-aggregation behavior of R-CM-chitosan

The solubility of R-CM-chitosan in aqueous solution was pH-dependent. The R-CM-chitosan samples were easily dissolved in water at pH 2.4–8.0, forming a limpid water dispersion. But the precipitation appeared in the R-CM-chitosan water dispersion when pH > 8.0.

The critical micellar concentration (cmc) of R-CM-chitosan was determined by intensity of dynamic light scattering (DLS) of the samples. When the concentration of R-CM-chitosan in water dispersion approached the cmc, higher intensity of DLS was detected and the Tyndall phenomenon was observed clearly, as shown in Fig. 4, the cmc of R-CM-chitosan was 0.20 mg/ml, which was smaller than R-Na 0.40 mg/ml.

3.5. Effect of concentration factor on nanoparticles size, PDI and zeta potential

Aza/R-CM-chitosan particle size, PDI and zeta potential were measured by dynamic light scattering (DLS) under varying concentrations of the carrier and the drug. The results are listed in Table 3. In brief, the particle sizes ranged between 100 and 800 nm, with the PDIs being essentially less than 0.70. The smaller the PDI, the better the observed uniformity of the particles (Donini, Robinson,

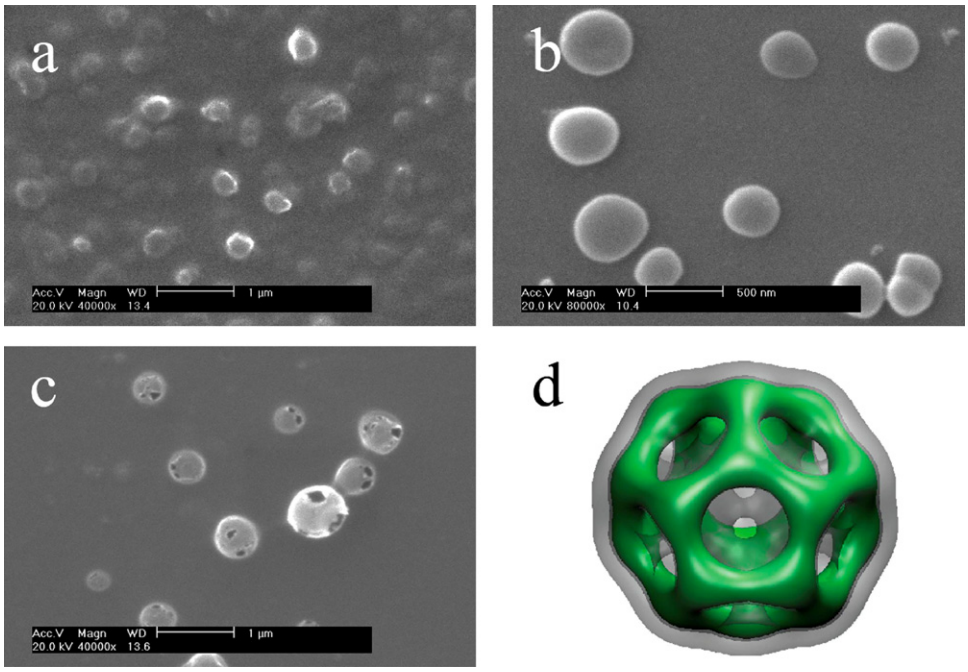

Fig. 2. SEM photos of Aza/R-CM-chitosan nanoparticles, (a) [R-CM-chitosan]/[Aza] = 5, (b) [R-CM-chitosan]/[Aza] = 15, (c) [R-CM-chitosan]/[Aza] = 5, drying at 60 °C, (d) simulation graph of polymers cage-shaped micelle.

Colombo, Giordano, & Peppas, 2002). Since carboxymethyl groups trended to the water phase as expected, zeta potential data in Table 3 indicated the surface charge of particles were correspondingly negative.

In the Aza/R-CM-chitosan water dispersion, the particle size could be regulated by varying the carrier or the drug concentrations. The minimum particle size was 131.5 nm and was achieved at lower R-CM-chitosan and Aza concentrations (Table 3). When the concentration of R-CM-chitosan was increased from 0.1 to 0.9 mg/ml while the concentration of Aza was kept constant, the resulting particles were larger. The particles size increased (846.3 nm) when the Aza concentration was increased to 0.05 mg/ml and the concentration of R-CM-chitosan was held constant.

There was an approximately linear relationship between the ability to solubilize drugs and the micelle size that usually increased with increased concentration of the polymer carrier (Chen, Zhang, & Guo, 2006; Kitahara, Tamai, & Hayano, 1991). A higher carrier concentration meant the addition of more hydrophobic R groups, which resulted in better compatible between the R-CM-chitosan and the Aza when the Aza concentration was held constant (Shen, 2002). Meanwhile, Aza would trend toward the hydrophobic

Table 3
Particles size, PDI and zeta potential under varying concentrations of R-CM-chitosan and Aza (pH = 6.8).

R-CM-chitosan [mg/ml]	Aza [mg/ml]	Particle size [nm]	PDI	Zeta potential [mV]
0.10	0.02	307.6 ± 22.5	0.527 ± 0.0023	−4.77 ± 3.1
0.10	0.05	474.9 ± 26.0	0.610 ± 0.0020	−5.19 ± 3.9
0.10	0.1	502.4 ± 32.6	0.561 ± 0.0033	−11.8 ± 3.5
0.10	0.15	264.4 ± 21.8	0.411 ± 0.0019	−24.4 ± 3.6
0.10	0.2	242.1 ± 20.0	0.497 ± 0.0024	−28.5 ± 3.6
0.30	0.02	134.7 ± 9.8	0.282 ± 0.0014	−24.1 ± 4.5
0.30	0.05	158.3 ± 17.6	0.997 ± 0.0010	−32.4 ± 4.5
0.30	0.1	481.2 ± 24.2	0.590 ± 0.0026	−29.2 ± 3.5
0.30	0.15	375.4 ± 24.9	0.512 ± 0.0023	−44.9 ± 10.9
0.30	0.2	131.5 ± 6.6	0.675 ± 0.0030	−40.1 ± 3.7
0.50	0.02	276.8 ± 22.6	0.321 ± 0.0015	−14.7 ± 3.0
0.50	0.05	276.1 ± 18.9	0.997 ± 0.0010	−42.6 ± 4.6
0.50	0.1	372.4 ± 29.1	0.700 ± 0.0040	−34.5 ± 3.3
0.50	0.15	534.0 ± 39.0	0.647 ± 0.0034	−39.2 ± 3.3
0.50	0.2	145.4 ± 7.8	0.598 ± 0.0024	−30.5 ± 4.0
0.70	0.02	231.6 ± 15.0	0.480 ± 0.0023	−16.3 ± 4.9
0.70	0.05	549.5 ± 28.4	0.608 ± 0.002	−41.8 ± 3.3
0.70	0.1	474.1 ± 37.4	0.888 ± 0.0045	−42.1 ± 3.9
0.70	0.15	433.0 ± 34.4	0.741 ± 0.0040	−43.7 ± 3.8
0.70	0.2	221.4 ± 12.3	0.505 ± 0.0023	−24.4 ± 3.5
0.90	0.02	381.0 ± 29.3	0.337 ± 0.0020	−11.7 ± 2.2
0.90	0.05	846.3 ± 58.7	0.591 ± 0.0010	−35.6 ± 4.2
0.90	0.1	802.9 ± 56.5	0.675 ± 0.0037	−28.8 ± 2.5
0.90	0.15	577.3 ± 29.8	0.895 ± 0.0038	−22.4 ± 1.3
0.90	0.2	540.7 ± 26.8	0.895 ± 0.0046	−31.8 ± 3.5

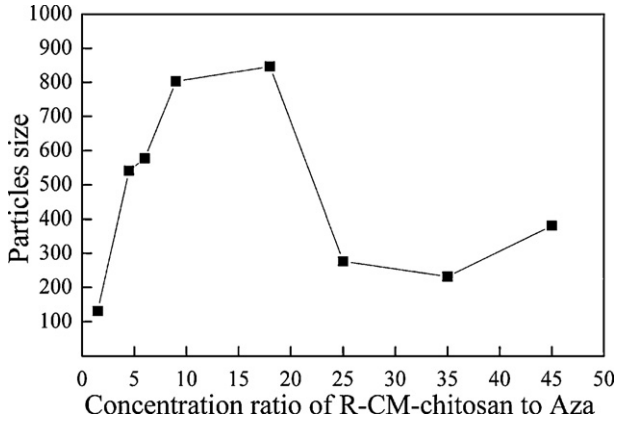

Fig. 3. Effect of [R-CM-chitosan]/[Aza] on particles size.

domain in R-CM-chitosan micelle, which became a solubilized micelle. Furthermore, according to the steric stabilization theory, coverage of R-CM-chitosan would reduce interfacial energy between Aza and water, which could increase the stability of the water dispersion. The interfacial energy mentioned could also be lowered by increasing the Aza concentration while keeping the R-CM-chitosan concentration constant. However, a increase in particle size only occurred when the ratio of the carrier to the drug was less than 20 (Fig. 3). When the R-CM-chitosan concentration increased, the forces among micelles, surface molecules of micelles and solution molecules would dramatically increase also. Thus bigger micelles would disaggregate to much smaller ones to decrease the free energy of mixing (Kitahara et al., 1991). The particle size was reduced correspondingly, which was also shown in Fig. 3 when the ratio of the carrier to the drug was more than 20.

Aza/R-CM-chitosan particle size at nanoscale level could be controlled by adjusting the concentration ratio of R-CM-chitosan to Aza. Additionally, the PDI of the particles should be less than 0.70 to maintain a uniform particle size and improved bioavailability of pesticide. As the Aza concentration remained constant, and the PDI became much bigger as the R-CM-chitosan concentration increased (Table 3). For example, R-CM-chitosan concentration increased from 0.1 mg/ml to 0.9 mg/ml while the PDI increased from 0.411 to 0.895, which was close to the PDI of polydispersed nanoparticles. When the ratio of the carrier to the drug was more than 10, the PDI decreased rapidly as the ratio increased.

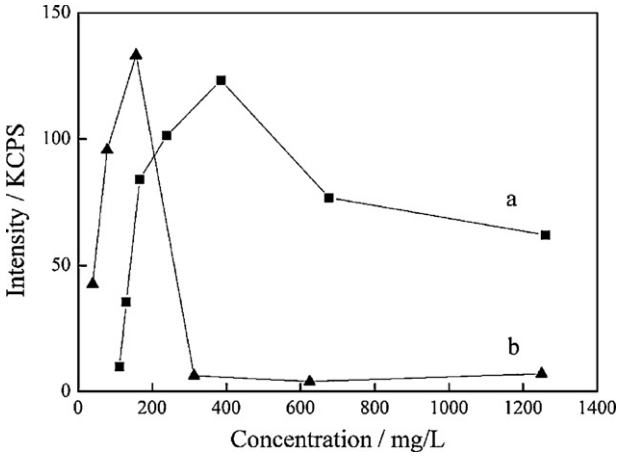

Fig. 4. The intensity of light scattering of RA-Na(a) and CMC-g-RA(b) in water.

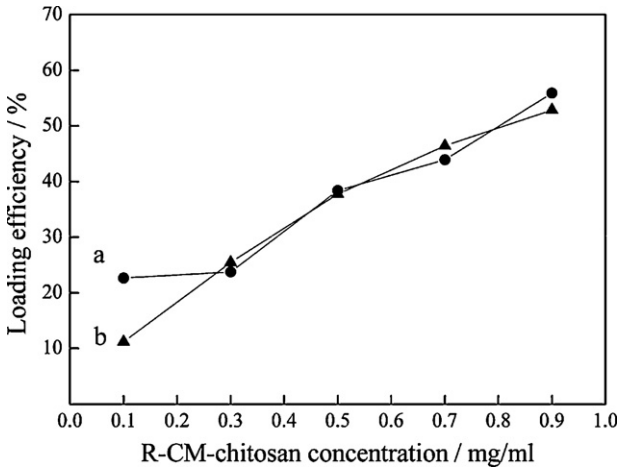

Fig. 5. Aza LE of Aza/R-CM-chitosan, [Aza] = 0.05 mg/ml (a) and [Aza] = 0.10 mg/ml (b).

Zeta potential was also influenced by the concentration ratio of R-CM-chitosan to Aza (Table 3). A higher zeta potential, usually >30 mV, indicated a stronger electrostatic repulsive force that was beneficial to maintain steady water dispersion (Li et al., 2007). When the ratio of the carrier to the drug was less than 15, zeta potential increased rapidly with the ratio increasing. One of the maximum observed zeta potentials was −42.6 mV, which occurred when the concentrations of R-CM-chitosan and Aza were 0.50 mg/ml and 0.05 mg/ml, respectively (Table 3). One reason for this was that more carboxymethyl groups with a negative charge were added to the water dispersion when the carrier concentrations were increased. On the other hand, increased Aza concentrations, lead to the stronger affinity of the hydrophobic groups in the carrier and the drug, which also resulted in more carboxymethyl groups specifically trended toward the water phase (Shen, 2002).

When the ratio of the carrier to the drug was less than 6, surface tensions, contact angles and zeta potential also increased with the ratio increasing (Table 4). And the surface tensions and contact angles of Aza/R-CM-chitosan water dispersion decreased slowly after the ratio being larger than 10. The smallest surface tension and contact angle of the R-CM-chitosan without loading Aza was 42.5 mN/m and 58.7°, respectively, as shown in Table 4. Thus higher concentration ratio of R-CM-chitosan to Aza tended to bring about great wettability.

According to measurements of the particle size, the PDI, the zeta potential, surface tension and contact angle of the Aza/R-CM-chitosan water dispersion, a stable and uniform nanoparticle water-dispersion could be obtained when the concentration ratio of R-CM-chitosan to Aza was regulated between 5 and 15.

3.6. LE of Aza/R-CM-chitosan particle

The Aza standard's retention time was 7.9 min after HPLC test (Wu et al., 2005), and loading efficiency (LE) of Aza/R-CM-chitosan samples could be calculated by the following equation, where A stood for the total Aza concentration and B represented the concentration of free Aza in the supernatant.

$$\frac{\text{LE of cap}}{\text{R-CM-chitosan}} = \frac{A-B}{A-B}A \times 100\%$$

When the Aza concentration of the Aza/R-CM-chitosan samples was 0.05 mg/ml, LE increased from 23% to 56% with an increasing R-CM-chitosan concentration (Fig. 5a), where the concentration ratio

Table 4
Aza/R-CM-chitosan surface tensions, contact angles and zeta potentials under varying concentrations of R-CM-chitosan and Aza (pH = 6.8).

R-CM-chitosan [mg/ml]	Aza [mg/ml]	γ [mN/m]	Contact angles [°]	Zeta potential [mV]
0.10	0.05	46.9	63.0 ± 4.2	−5.19 ± 3.9
0.10	0.1	43.6	63.6 ± 8.6	−11.8 ± 3.5
0.30	0.05	50.2	81.6 ± 3.2	−32.4 ± 4.5
0.30	0.1	47.4	75.2 ± 2.0	−29.2 ± 3.5
0.50	0.05	46.6	73.2 ± 5.6	−42.6 ± 4.6
0.50	0.1	50.0	81.2 ± 2.3	−34.5 ± 3.3
0.70	0.05	45.7	70.6 ± 6.7	−41.8 ± 3.3
0.70	0.1	47.8	76.2 ± 4.4	−42.1 ± 3.9
0.90	0.05	46.3	72.4 ± 7.0	−35.6 ± 4.2
0.90	0.1	47.5	78.0 ± 3.8	−28.8 ± 2.5
1.0	0	42.5	58.7 ± 5.7	−41.2 ± 2.2

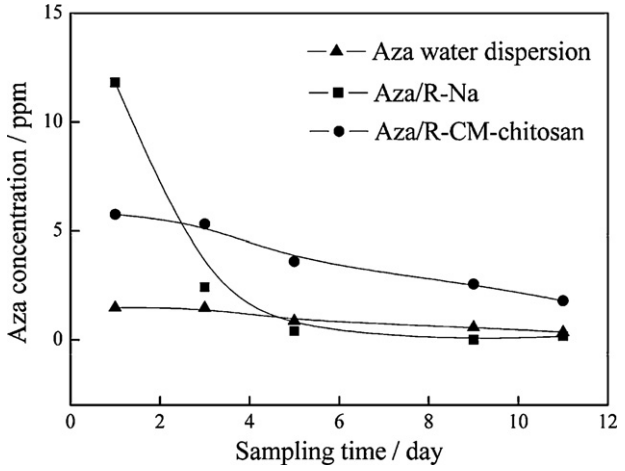

Fig. 6. Aza concentrations under sampling times in leaching liquors.

of R-CM-chitosan to Aza was about 2–18. The similar linear varying trend was observed in particles sizes (Fig. 3), where the band value of LE corresponded to [R-CM-chitosan]/[Aza] = 18. When the Aza concentration was 0.10 mg/ml (Fig. 5b), the LE increased from 11% to 53% with an increased R-CM-chitosan concentration that coincided with a [R-CM-chitosan]/[Aza] < 10 (Fig. 3).

3.7. Outdoor stability of Aza/R-CM-chitosan water dispersion

Stability of the Aza/R-CM-chitosan water dispersion was evaluated by measuring the residual Aza concentrations at specific sampling times remaining in the leaching liquid. Samples ([R-CM-chitosan]/[Aza] = 5, where [R-CM-chitosan] = 0.50 mg/ml, [Aza] = 0.10 mg/ml) with a LE of 53% (Fig. 6) were chosen and compared with Aza/R-Na and the Aza water dispersion samples that were used as the control groups. During 11 days of outdoor testing, the residual Aza concentration of Aza/R-CM-chitosan sample was higher than that of the control groups (Fig. 6). In the first 3 days, the Aza concentration in the Aza/R-CM-chitosan sample slowly decreased from about 5.7 ppm to 5.3 ppm, at the same time, the control groups curves dropped quickly. After 4 days the residual Aza concentrations were about 3.6–1.8 ppm in the Aza/R-CM-chitosan sample. Thus, the polymer carrier R-CM-chitosan efficiently restrained the Aza degradation compared to the control groups. The high LE of the Aza/R-CM-chitosan implied that the unloaded Aza molecules were seldom outside micelles, hence the Aza concentration decreased relatively slower than that in control groups. The polymer carrier also provided much effective protection for the Aza compared to a small molecule carrier (R-Na) or no carrier (water). Thus, the carrier R-CM-chitosan provided a slow and stable method to release Aza at high concentrations.

4. Conclusions

The novel drug carrier R-CM-chitosan was synthesized under mild conditions. The lipid-soluble group R reacted with the water-soluble CM-chitosan molecule. The amphiphilic R-CM-chitosan turned into a polymeric micellar self-assembly in water, which became an efficient drug carrier for the lipid-soluble pesticide, Aza. The Aza/R-CM-chitosan water dispersion was prepared by blending the carrier and the drug together. Aza/R-CM-chitosan particles were nanoscale smooth spheres. The small-size of the nanoparticles could improve infiltration and bioavailability of Aza. Adjusting concentrations ratios of R-CM-chitosan to Aza, especially [R-CM-chitosan]/[Aza] = 5–15, produced nanoparticles of a smaller, uniform particle size with a higher zeta potential. Aza was protected efficiently by the carriers while in micelles, and the highest LE of the Aza/R-CM-chitosan was 56% when [R-CM-chitosan]/[Aza] = 18. Therefore, Aza was stable and was released over the course of 11 days in the environment. This study provides chemical means to produce a non-toxic carrier that efficiently helps dissolve the lipid-soluble pesticide Aza into water. This would contribute to developing a green and safe botanical pesticide water dispersion formulation at the nanoscale level.

Acknowledgements

This project is supported by China National Natural Science Foundation (30771419 and 30971915). The authors thank the Polymers Laboratory in the Department of Materials Science and Engineering at Jinan University for supporting this work. We also thank Zi-Yong Zhang for his guidance.

References

Chen, T., Zhang, X. H., & Guo, R. (2006). Surface activity and aggregation of chitosan. *Acta Physico-chimica Sinica*, *16*, 1039–1402.
Donini, C., Robinson, D. N., Colombo, P., Giordano, F., & Peppas, N. A. (2002). Preparation of P (MAA-g-EG) nanospheres for pharmaceutical applications. *International Journal of Pharmaceutics*, *245*, 83–91.
Ge, H. C., & Luo, D. K. (2005). Preparation of carboxymethyl chitosan in aqueous solution under microwave irradiation. *Carbohydrate Research*, *340*, 1351–1356.
Guan, H. N., Chi, D. F., Yu, J., & Li, X. C. (2008). A novel photodegradable insecticide: Preparation, characterization and properties evaluation of nano-imidacloprid. *Pesticide Biochemistry and Physiology*, *92*, 83–91.
He, X. H., & Schmid, F. (2008). Spontaneous formation of complex micelles from a homogeneous solution. *Physical Review Letters*, *100*, 137802-1-4.
Kitahara, H. M., Tamai, Y. K., & Hayano, S. G. (1991). *Surfactant-property applications and chemecology*. Beijing: Chemical Industry Press., pp. 1–126.
Li, L., Xu, X. Y., & Zhou, J. P. (2007). Preparation and characterization of N-octyl-N'-succinyl chitosan micelles. *Chinese Journal of New Drugs*, *16*, 543–547.
Liu, Y., Tong, Z., & Prud'homme, R. K. (2008). Stabilized polymeric nanoparticles for controlled and efficient release of bifenthrin. *Pest Management Science*, *64*, 808–812.
Muzzarelli, R. A. A., Boudrant, J., Meyer, D., Manno, N., DeMarchis, M., & Paoletti, M. G. (2011). Current views on fungal chitin/chitosan, human chitinases, food preservation, glucans, pectins and inulin: A tribute to *Henri Braconnot*, precursor

of the carbohydrate polymers science, on the chitin bicentennial. *Carbohydrate Polymers*,. DOI information: 10.1016/j.carbpol.2011.09.063.
Nishimura, S. I., Nishi, N., & Tokura, S. (1986). Bioactive chitin derivatives: Activation of mouse peritoneal macrophages by o-carboxymethyl chitins. *Carbohydrate Research*, *146*, 251–258.
Shen, X. M., & Song, Y. (2009). Application of domestic novel surfactant in water-based pesticide. *Journal of China Agrochemicals*, *8*, 29–34.
Shen, Y. D. (2002). *Polymer surfactant*. Beijing: Chemical Industry Press., p. 107.
Shenoy, D. B., & Sukhorukov, B. (2004). Engineered microcrystals for direct surface modification with layer-by-layer technique for optimized dissolution. *European Journal of Pharmaceutics and Biopharmaceutics*, *58*, 521–527.
Wu, Y. K., Su, P. J., Zhang, Z., & Lin, J. (2005). Analysis of 0.3% azadirachtin emulsion by HPLC. *Yunnan Chemical Technology*, *32*, 35–37.
Yi, Y., Yang, H., Ying, G. Q., Chen, J. S., & Wang, H. (2006). Synthesis and properties of N-phthaloyl-chitosan. *Chemical Industry and Engineering Progress*, *25*, 542–545.